Constraints on T-odd and P-even hadronic interactions from nucleon, nuclear, and atomic electric dipole moments

W. C. Haxton and Antje Höring
Institute for Nuclear Theory, NK-12 and Department of Physics, FM-15, University of Washington, Seattle, Washington 98195

M. J. Musolf
Continuous Electron Beam Accelerator Facility Theory Group, MS 12H, Newport News, Virginia 23606 and Department of Physics, Old Dominion University, Norfolk, Virginia 23529
(Received 3 March 1994)

We deduce constraints on time-reversal-noninvariant (TRNI), parity-conserving (PC) hadronic interactions from nucleon, nuclear, and atomic electric dipole moment (EDM) limits. Such interactions generate EDM's through weak radiative corrections. We consider long-range mechanisms, i.e., those mediated by meson exchanges in contrast with short-range two-loop mechanisms. We find that the ratio of typical TRNI, PC nuclear matrix elements to those of the strong interaction are $\lesssim 10^{-5}$, a limit about 2 orders of magnitude more stringent than those from direct detailed balance studies of such interactions. This corresponds to a bound of $|\bar{g}_\rho| \lesssim 10^{-3}$, where $\bar{g}_\rho$ is a TRNI PC ρNN coupling.

PACS number(s): 13.40.Em, 11.30.Er, 24.80.−x, 35.10.Di

I. INTRODUCTION

Time-reversal-noninvariant (TRNI), parity-nonconserving (PNC) interactions arise naturally in the minimal standard model through the Kobayashi-Maskawa phase and through the θ term. Additional possibilities exist in extended models with left-right symmetry, more complicated Higgs sectors, etc. [1]. Experimental constraints on such interactions are often very stringent; for example, the neutron and atomic electric dipole moment limits on $|\theta|$ are about $\lesssim 10^{-10}$. In contrast, fundamental TRNI parity-conserving (PC) interactions do not arise in the standard model. In fact, it has been argued generally that, in renormalizable gauge models with elementary quarks, flavor-conserving TRNI PC interactions between quarks do not arise in first order in the boson exchanges between fermions. Such interaction could be generated, e.g., through weak corrections to TRNI PNC interactions [2]. Consequently, one expects such induced interactions to be extremely weak.

Despite this expectation, direct experimental constraints on TRNI PC interactions are relatively weak. For instance, compound nucleus studies of detailed balance and nuclear energy-level fluctuations yield $\alpha \lesssim 2 \times 10^{-3}$, where α measures the magnitude of typical TRNI PC nuclear matrix elements relative to those of the residual strong interaction [3–5]. A neutron transmission experiment [6] measuring the TRNI PC fivefold correlation

$$\boldsymbol{\sigma} \cdot (\mathbf{k} \times \mathbf{I})(\mathbf{k} \cdot \mathbf{I}) \ , \tag{1}$$

where $\boldsymbol{\sigma}$ and $\mathbf{k}$ are the neutron spin and momentum and $\mathbf{I}$ the nuclear spin, produced a similar limit, $\alpha \lesssim 5 \times 10^{-3}$.

Another set of constraints on TRNI PC interactions are indirect, namely, those extracted from TRNI PNC observables: Weak corrections to TRNI PC interactions can generate TRNI PNC observables, so that constraints on the former may be obtained from measurements of the latter. The extraordinary precision of TRNI PNC limits, such as those obtained in neutron and atomic electric dipole moment searches, results in interesting constraints on TRNI PC interactions, despite the need for the weak interaction. For instance, dimensional arguments suggest that the neutron electric dipole moment (EDM) bound requires TRNI PC meson-nucleon couplings to be $\lesssim 10^{-4}$ [7].

In this paper we will attempt to quantify neutron and atomic EDM limits on long-range TRNI PC nucleus-nucleus interactions [8]. By "long-range" we mean that the mechanism generating the EDM involves hadronic distance scales typical of meson exchange. Such interactions can then be described in terms of effective meson-nucleon couplings (either TRNI and PC or weak, PNC). This approach allows us to quantitatively compare such constraints with those direct tests of TRNI PC interactions in compound nuclei and/or with slow neutrons. Of course, the effective meson-nucleon couplings are presumably generated from short-range boson exchanges between quarks, in analogy with the more familiar case of hadronic PNC [9].

We will discuss atomic EDM's generated from TRNI PC nuclear interactions in combination with Z^0 exchange between electrons and the nucleus, and the neutron and nuclear EDM's produced from such TRNI PC interactions in combination with hadronic weak meson-nucleon

couplings. We find that EDM limits on TRNI PC interactions are typically about 2 orders of magnitude more stringent than those deduced from compound nucleus studies, that is, $\alpha \lesssim 10^{-5}$. (The corresponding limit on the strength of a TRNI PC ρNN coupling is $|\bar{g}_\rho| \lesssim 10^{-3}$.) We also compare our results to the estimates by Conti and Khriplovich [10] of representative short-range two-loop contributions to nucleon EDM's.

II. TRNI PC AND TRI PNC NN INTERACTIONS

The weak PNC hadronic NN interaction at low energies is conventionally described in terms of meson exchange, where one meson-nucleon coupling is strong and the other weak. The validity of this description rests in part on the success of meson exchange models in describing strong NN interactions at low energies ($E < 300$ MeV), and in part on the observation that a sufficiently general PNC meson-exchange potential will generate the five possible S-P partial wave amplitudes ($^3S_1 \leftrightarrow {}^1P_1$ $\Delta I = 0$, $^1S_0 \leftrightarrow {}^3P_0$ $\Delta I = 0,1,2$, and $^3S_1 \leftrightarrow {}^3P_1$ $\Delta I = 1$). Thus one can think of the meson-exchange description both as a bookkeeping device for the most general elementary amplitude governing the long-wavelength PNC components in nuclear wave functions and as a model for extrapolating those amplitudes to higher energies. These amplitudes, and by inference the meson-nucleon couplings, have been constrained by a number of PNC experiments in NN, few-nucleon, and nuclear systems [11]. While in principle they could be calculated from the standard electroweak model, hadronic effects dress the elementary W and Z exchanges occurring within the vertices in a complicated way. Consequently, standard model estimates [9] of meson-nucleon PNC couplings are typically assigned an uncertainty of factors of $\pm(1$–$3)$.

The standard form of the meson exchange weak NN potential can be calculated from the strong and PNC weak couplings [9,12]:

$$H^{\rm PC} = -ig_{\pi NN}\bar{N}\gamma_5\boldsymbol{\tau}\cdot\boldsymbol{\phi}_\pi N + g_\rho\bar{N}\left(\gamma_\mu + i\frac{\mu_v}{2M}\sigma_{\mu\nu}k^\nu\right)\boldsymbol{\tau}\cdot\boldsymbol{\phi}_\rho^\mu N + g_\omega\bar{N}\left(\gamma_\mu + i\frac{\mu_s}{2M}\sigma_{\mu\nu}k^\nu\right)\phi_\omega^\mu N\ , \tag{2a}$$

$$H^{\rm PNC} = \frac{f_\pi}{\sqrt{2}}\bar{N}(\boldsymbol{\tau}\times\boldsymbol{\phi}_\pi)_z N - \bar{N}\left(h_\rho^0\boldsymbol{\tau}\cdot\boldsymbol{\phi}_\rho^\mu + h_\rho^1\phi_{\rho z}^\mu + \frac{h_\rho^2}{2\sqrt{6}}(3\tau_z\phi_{\rho z}^\mu - \boldsymbol{\tau}\cdot\boldsymbol{\phi}_\rho^\mu)\right)\gamma_\mu\gamma_5 N - \bar{N}(h_\omega^0\phi_\omega^\mu + h_\omega^1\tau_z\phi_\omega^\mu)\gamma_\mu\gamma_5 N\ . \tag{2b}$$

This yields the π-, ρ-, and ω-exchange NN potential [9,11]

$$\begin{aligned} V^{\rm PNC}(\mathbf{r}) = {} & \frac{iF_\pi}{M}[\tau(1)\times\tau(2)]_z[\boldsymbol{\sigma}(1)+\boldsymbol{\sigma}(2)]\cdot\mathbf{u}_\pi(\mathbf{r}) \\ & + \frac{1}{M}\left(\left\{F_0\boldsymbol{\tau}(1)\cdot\boldsymbol{\tau}(2) + \frac{F_1}{2}[\boldsymbol{\tau}(1)+\boldsymbol{\tau}(2)]_z + \frac{F_2}{2\sqrt{6}}[3\tau(1)_z\tau(2)_z - \boldsymbol{\tau}(1)\cdot\boldsymbol{\tau}(2)]\right\}\right. \\ & \times\{(1+\mu_v)i[\boldsymbol{\sigma}(1)\times\boldsymbol{\sigma}(2)]\cdot\mathbf{u}_\rho(\mathbf{r}) + [\boldsymbol{\sigma}(1)-\boldsymbol{\sigma}(2)]\cdot\mathbf{v}_\rho(\mathbf{r})\} + \left\{G_0 + \frac{G_1}{2}[\boldsymbol{\tau}(1)+\boldsymbol{\tau}(2)]_z\right\} \\ & \times\{(1+\mu_s)i[\boldsymbol{\sigma}(1)\times\boldsymbol{\sigma}(2)]\cdot\mathbf{u}_\omega(\mathbf{r}) + [\boldsymbol{\sigma}(1)-\boldsymbol{\sigma}(2)]\cdot\mathbf{v}_\omega(\mathbf{r})\} \\ & \left. + \frac{1}{2}[\boldsymbol{\tau}(1)-\boldsymbol{\tau}(2)]_z[\boldsymbol{\sigma}(1)+\boldsymbol{\sigma}(2)]\cdot[G_1\mathbf{v}_\omega(\mathbf{r}) - F_1\mathbf{v}_\rho(\mathbf{r})]\right) \end{aligned} \tag{3}$$

when $\mathbf{r} = \mathbf{r}_1 - \mathbf{r}_2$, $u = [\mathbf{p}_1 - \mathbf{p}_2, e^{-mr}/4\pi r]$, and $v = \{\mathbf{p}_1 - \mathbf{p}_2, e^{-mr}/4\pi r\}$, and where the strong scalar and vector magnetic moments are assigned their vector dominance values $\mu_s = -0.12$ and $\mu_v = 3.70$. The $\Delta I = 1$ pion exchange strength F_π, the $\Delta I = 0$, 1, and 2 ρ exchange strengths F_0, F_1, and F_2, and the $\Delta I = 0$ and 1 ω exchange strengths G_0 and G_1 are given as products of weak and strong meson couplings in Table I. A fit to pp, few-body, and nuclear PNC observables yields $F_0 \sim 10^{-6}$ and $F_\pi \lesssim 0.4\times10^{-6}$ [11].

TABLE I. Weak coupling constants and "best value" and "reasonable range" standard model values of Ref. [11].

Coefficient	Equivalent	Best value (10^{-6})	Reasonable range (10^{-6})
F_π	$g_{\pi NN}f_\pi/\sqrt{32}$	1.08	0:2.71
F_0	$-g_\rho h_\rho^0/2$	1.59	−1.59:4.29
F_1	$-g_\rho h_\rho^1/2$	0.027	0:0.053
F_2	$-g_\rho h_\rho^2/2$	1.33	−1.06:1.54
G_0	$-g_\omega h_\omega^0/2$	0.80	−2.39:4.29
G_1	$-g_\omega h_\omega^1/2$	0.48	0.32:0.80

Similarly, the general structure of TRNI PC NN interactions has been discussed by Herczeg [13] and by Simonius [14]. The lowest allowed partial waves are the $\Delta I = 0$ ${}^3S_1 \leftrightarrow {}^3D_1$ and $\Delta I = 1$ ${}^1P_1 \leftrightarrow {}^3P_1$ amplitudes, and these should dominate TRNI PC interactions at nuclear length scales. Simonius discussed the most general single-meson-exchange model for such interactions. As no scalar-pseudoscalar exchanges are allowed, no pion-range interaction exists. The spin and isospin structure of $J \neq 0$ normal parity exchanges is unique: the isospin-operator is the isovector $(\boldsymbol{\tau}_1 \times \boldsymbol{\tau}_2)_z$, corresponding to charged mesons, and the permitted spin-orbit structures are the singlet-triplet transitions ${}^1P_1 \leftrightarrow {}^3P_1$, ${}^1D_2 \leftrightarrow {}^3D_2$, etc. The longest ranged TRNI PC vector meson exchange is thus $\rho^{\pm}$. The strong ρNN vertex is given by Eq. (2a), while the TRNI vertex is

$$H^{\mathrm{TRNI}} = -\bar{g}_\rho g_\rho \bar{N} \frac{\mu_v}{2M} \sigma_{\mu\nu} k^\nu \sqrt{2} (\tau_- \phi_+^{\mu *} - \tau_+ \phi_-^{\mu *}) N \ . \quad (4)$$

ρ-meson exchange then generates the nonrelativistic TRNI PC NN potential [14]

$$V_\rho(\mathbf{r}) = \frac{m_\rho^3}{M^2} g_\rho^2 \bar{g}_\rho \frac{\mu_v}{4\pi} [\boldsymbol{\tau}(1) \times \boldsymbol{\tau}(2)]_3 \frac{e^{-m_\rho r}}{m_\rho^3 r^3} \times (1 + m_\rho r)(\boldsymbol{\sigma}_1 - \boldsymbol{\sigma}_2) \cdot \boldsymbol{l} \ , \quad (5)$$

where the strong coupling $g_\rho = 2.79$ and where $\bar{g}_\rho$ parametrizes the strength of the TRNI vertex. The angular momentum operator $\boldsymbol{l} = \mathbf{r} \times (\mathbf{p}_1 - \mathbf{p}_2)/2$. This potential contributes to the pn interaction only.

For $J \neq 0$ unnatural parity exchanges all allowed TRNI PC partial wave amplitudes can contribute (${}^3S_1 \leftrightarrow {}^3D_1$, ${}^1P_1 \leftrightarrow {}^3P_1$, ${}^1D_2 \leftrightarrow {}^3D_2$, ${}^3P_2 \leftrightarrow {}^3F_2$, etc.). Various authors have discussed the potential generated by A_1 exchange [15].

In this paper we adopt the Simonius ρ-exchange potential [Eq. (5)] as a representative phenomenological TRNI PC interaction. This selection is made because it is the longest range meson-exchange interaction, and for reasons of simplicity. [Note that the inclusion of the A_1 would produce a potential analogous to Eq. (3), fully general in the long-wavelength limit.]

III. LONG-RANGED CONTRIBUTIONS TO THE NEUTRON, NUCLEAR, AND ATOMIC ELECTRIC DIPOLE MOMENTS

TRNI PC interactions in combination with the weak interaction can generate TRNI PNC observables. It has long been appreciated that the stringent limits on neutron and atomic EDM's must then impose important limits on TRNI PC interactions. In this paper we extract such limits by studying long-range mechanisms generating EDM's, i.e., mechanisms involving meson exchange length scales in nuclei or the neutron. The limits we obtain on the TRNI PC meson-nucleus coupling $\bar{g}_\rho$ are translated into a bound on α, the ratio of typical TRNI PC and strong nuclear matrix elements, so that a comparison to direct tests of TRNI in compound nuclei can be made.

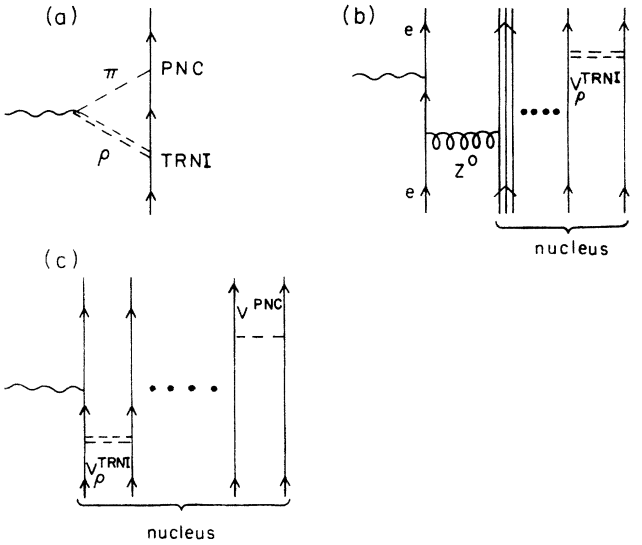

FIG. 1. Schematic representations of (a) the π-ρ loop contribution to the nucleon EDM, (b) the atomic EDM generated by Z exchange between the electrons and nucleons in combination with a polarizing TRNI ρ potential in the nucleus, and (c) the nuclear EDM generated by the simultaneous polarization of the nucleus by TRNI ρ and PNC π potentials.

We stress that, although the interactions we study occur at meson-exchange length scales, the physics which generates $\bar{g}_\rho$ can involve very short distances (e.g., TRNI quark-quark interactions mediated by heavy vector-boson exchange). Attempts to compute $\bar{g}_\rho$ using fundamental interactions at the level of quarks involves a considerable degree of theoretical uncertainty—a consequence of the present lack of reliable methods for computing low-energy hadronic four (or more) quark operator matrix elements from first principles in QCD. Thus, we treat $\bar{g}_\rho$ as an effective parameter which (i) characterizes long-distance interactions induced by short-distance TRNI physics, and (ii) may be used to compare constraints from competing experiments. We note also that short-range physics may, in general, generate EDM mechanisms which cannot be represented in terms of meson exchange and effective meson-nucleon TRNI PC couplings. Examples of such short-ranged EDM mechanisms have been recently considered by Conti and Khriplovich, who claim very stringent limits [10]. We will discuss these limits and the comparison with the present work in our conclusions.

The experimental limits on the neutron and atomic electric dipole moments have reached remarkable sensitivity. The two-standard-deviation upper bound on the magnitude of the neutron EDM is 8×10^{-26} e cm [16,17], while the limit on the atomic EDM of ^{199}Hg is $d_A \lesssim 1.3 \times 10^{-27}$ e cm (95% C.L.) [18]. In this paper we evaluate three EDM mechanisms, the meson-cloud contribution to the EDM of the nucleon, the nuclear EDM that arises from the simultaneous polarization of the nucleus by the PNC weak and PC TRNI interactions, and the atomic EDM that arises from a PC TRNI interaction in the nucleus in combination with Z exchange between the nucleus and the atomic electrons. These mechanisms are represented schematically in Fig. 1. The re-

sulting comparisons to the experimental limits then provide bounds on $\bar{g}_\rho$ and, equivalently, α.

IV. THE NEUTRON EDM

Dimensional estimates have been made of the constraints the neutron EDM, induced by weak radiative corrections, places on TRNI PC meson-nucleon couplings [7]. We have made such estimates more quantitative by evaluating the meson-cloud contribution to the EDM in a model where the TRNI is generated by the ρNN coupling $\bar{g}_\rho$. The calculated hadronic loop is depicted in Fig. 1(a), where for the weak hadronic coupling only f_π in Table I is retained. In principle, there exists a large number of additional diagrams dependent on $\bar{g}_\rho$ which also contribute, such as the loop where the pion in Fig. 1(a) is replaced by the ρ. However, we expect the amplitude associated with the loop in Fig. 1(a) to at least set the scale of, if not dominate over, all hadronic loops since it contains the lowest-mass meson: one naively expects the longest range interactions to produce the large charge separations that dominate the EDM.

In carrying out the loop calculation, one faces a choice of regularization scheme. For point hadron couplings, the loop integral is linearly divergent. One approach to regulating this divergence would be to adopt the field theoretic framework of chiral perturbation theory (CPT). However, as the loop contains no chiral singularities, higher-dimension operators appearing in the chiral Lagrangian could generate terms analytic in the meson masses which are as important as those arising from the loop. Since one has, at present, insufficient information to determine the coefficients of the higher-dimension chiral operators, the result of a CPT calculation would be ambiguous. An alternative approach, which we follow, is to treat the hadrons as extended objects and include form factors at the meson-nucleon vertices. While this approach is admittedly more model dependent than that of CPT, it allows one to incorporate experimental information on the physics of meson-nucleon vertices.

We introduce form factors at both meson-nucleon vertices, using the parametrization of Ref. [19]:

$$F(k^2) = \frac{m^2 - \Lambda^2}{k^2 - \Lambda^2} \ , \tag{6}$$

where k is the meson momentum and m its mass. The cutoff parameter was fit to baryon-baryon scattering by the Bonn group, which found 1.0 GeV$\lesssim \Lambda \lesssim$ 1.5 GeV. In general, the momentum dependence of the meson-nucleon vertices generates additional "seagull" interactions that must be included to preserve electromagnetic gauge invariance [20,21]. In the case of the $\rho - \pi$ loop of Fig. 1(a), however, seagull vertices make no contribution to the EDM.

The result of the loop integration is the EDM Lorentz structure

$$iM_\mu = id_n \bar{u}(p')\sigma_{\mu\nu}q^\nu\gamma_5 u(p) \ , \tag{7}$$

where $u(p)$ is the nucleon spinor and $q = p' - p$. The neutron EDM d_n is

$$d_n = \frac{e f_\pi g_{\rho\pi\gamma} g_\rho \bar{g}_\rho \mu_v}{16\sqrt{2}\pi^2 m_\rho} \tilde{F}(m_\pi, m_\rho, m_N, \Lambda) \ , \tag{8}$$

where $\tilde{F}$ is a complicated function of the masses and cutoff:

$$\begin{aligned}\tilde{F} = &-\frac{11}{6} - [3L_0^\Lambda - L_1^\Lambda - 2L_2^\Lambda] + \frac{2\bar{\Lambda}^2 - \bar{m}_\rho^2 - \bar{m}_\pi^2}{(\bar{\Lambda}^2 - \bar{m}_\rho^2)(\bar{\Lambda}^2 - \bar{m}_\pi^2)}[2L_3^\Lambda + (3 - 2\bar{\Lambda}^2)L_2^\Lambda - \bar{\Lambda}^2 L_1^\Lambda + 3\bar{\Lambda}^2 L_0^\Lambda] \\ &+ \frac{\bar{m}_\pi^2 - \bar{\Lambda}^2}{(\bar{m}_\rho^2 - \bar{\Lambda}^2)(\bar{m}_\pi^2 - \bar{m}_\rho^2)}[2L_3^{m_\rho} + (3 - 2\bar{m}_\rho^2)L_2^{m_\rho} - \bar{m}_\rho^2 L_1^{m_\rho} + 3\bar{m}_\rho^2 L_0^{m_\rho}] \\ &+ \frac{\bar{m}_\rho^2 - \bar{\Lambda}^2}{(\bar{m}_\rho^2 - \bar{m}_\pi^2)(\bar{m}_\pi^2 - \bar{\Lambda}^2)}[2L_3^{m_\pi} + (3 - 2\bar{m}_\pi^2)L_2^{m_\pi} - \bar{m}_\pi^2 L_1^{m_\pi} + 3\bar{m}_\pi^2 L_0^{m_\pi}]\end{aligned} \tag{9}$$

with $\bar{m} = m/M$ and $L_n^m \equiv \int_0^1 dx\, x^n \ln[x^2 + (1-x)\bar{m}^2]$. Evaluating this expression for $\Lambda = 1.4$ GeV and $g_{\rho\pi\gamma} = 0.4$ we find

$$d_n \sim 1.5 \times 10^{-22} \left(\frac{f_\pi}{f_\pi^{\rm DDH}}\right) \bar{g}_\rho \ e\,{\rm cm} \ , \tag{10}$$

where $f_\pi^{\rm DDH}$ is the calculated "best value" weak PNC πNN coupling of Ref. [11], and f_π is its physical value. The experimental bounds on the neutron EDM from the Grenoble [16] and Gatchina [17] experiments are $-(3 \pm 5) \times 10^{-26}\ e$ cm and $+(2.6 \pm 4.2 \pm 1.6) \times 10^{-26}\ e$ cm at 1σ, and the corresponding 2σ upper bounds are given [16,17] as $12 \times 10^{-26}\ e$ cm and $11 \times 10^{-26}\ e$ cm, respectively. We adopt, as the combined result,

$$|d_n| \lesssim 8 \times 10^{-26}\ e\,{\rm cm} \ .$$

We conclude

$$|\bar{g}_\rho| \lesssim 0.5 \times 10^{-3} \left|\frac{f_\pi^{\rm DDH}}{f_\pi}\right| \ . \tag{11}$$

Later we will show that limit translates into a bound on α, the ratio of TRNI nuclear matrix elements to that of the strong residual interaction, of $|\alpha| \lesssim 10^{-5}$, using $f_\pi = f_\pi^{\rm DDH}$. These bounds change by less than a factor of 2 as Λ is varied over the recommended range of Bonn-potential values.

The bound in Eq. (11) depends on the strength of the πNN PNC weak coupling, and for this reason can be evaded. This is because of the puzzling result, deduced primarily from measurements of the circular polarization of the 1081 keV γ ray from ^{18}F, that f_π is no more

than 1/3 of the expected "best value" estimate $f_\pi^{\rm DDH}$ of Donoghue, Desplanques, and Holstein [11]. On the other hand, we also expect that limits comparable to Eq. (11) could be deduced from diagrams similar to Fig. 1(a), but including different ρ- and π-meson loops. The isoscalar PNC ρNN coupling is known to be approximately of the expected strength, that is, near the best value of Ref. [9]. Consequently, we expect Eq. (11) to set the scale of neutron EDM limits on $\bar{g}_\rho$.

V. ATOMIC EDM'S ARISING FROM ATOMIC PNC [8]

Given a TRNI PC nuclear interaction, Z exchange between the nucleus and the atomic electrons can generate an atomic EDM [Fig. 1(b)]. The coupling of the exchanged Z^0 to the nucleus must be TRNI and PC, under the assumption that the nucleus remains in its ground state. Ground state expectation values linear in the TRNI amplitude can exist for odd multipoles of the axial charge operator ($C1^5, C3^5$, etc), even magnetic multipoles of the axial three-current ($M2^5, M4^5$, etc.), and even multipoles of the vector three-current ($E2, E4$, etc.). The electric multipoles vanish in leading order by Siegert's theorem leaving the spin-dependent pieces and higher-order corrections. Furthermore, the contributions of higher multipoles to the electron-nucleus interaction are typically suppressed by powers of (r_N/r_A), where r_N and r_A are the nuclear and atomic radii, since large angular momentum transfers produce unfavorable electron overlaps with the nucleus. One concludes that the electron-nucleus interaction will be dominated by the $C1_e \cdot C1_N^5$ dipole term, which is contained in the interaction

$$H = \frac{G_F}{\sqrt{2}} \int d\mathbf{x} \rho_e^V(\mathbf{x}) \rho_N^5(\mathbf{x}) \ , \tag{12}$$

where $\rho_e^V(\mathbf{x})$ is the electron vector charge density and $\rho_N^5(\mathbf{x})$ the nuclear axial charge density. For nonrelativistic nucleons the corresponding electron interaction generating $S \leftrightarrow P$ transitions is a contact interaction

$$H_{\rm eff}(\mathbf{x}) = -\frac{G_F}{\sqrt{2}} \frac{1}{4M} g_A (1 - 4\sin^2\theta_W) \frac{\langle \mathbf{I} \rangle}{I} \cdot \nabla \delta(\mathbf{x}) \left\langle \phi^{\rm GS}_{IM=I} \left| \sum_{i=1}^{A} \left[r_z \frac{1}{i} \boldsymbol{\sigma}_i \cdot \overrightarrow{\boldsymbol{\nabla}}_i - \frac{1}{i} \boldsymbol{\sigma}_i \cdot \overleftarrow{\boldsymbol{\nabla}}_i r_z \right] \tau_3(i) \right| \phi^{\rm GS}_{IM=I} \right\rangle \ , \tag{13}$$

where $g_A = 1.25$, θ_W is the Weinberg angle, $\mathbf{I}$ is the nuclear spin, $|\phi^{\rm GS}\rangle$ is the nuclear ground state, and the $C1_N^5$ matrix element is evaluated in the magnetic state $M = I$.

If $|\phi_0^{\rm GS}\rangle$ is the unperturbed TRI ground state, the nuclear matrix element in Eq. (13) can be written

$$\sum_n \left\langle \phi_0^{\rm GS} \left| V_\rho \frac{|I_n\rangle\langle I_n|}{E_0 - E_{I_n}} C1_N^5 \right| \phi_0^{\rm GS} \right\rangle + \text{H.c.} \ , \tag{14}$$

where the sum extends over a complete set of nuclear excited states. To evaluate this expression we employ a trick frequently used in studies of nuclear PNC, the replacement of a many-body operator by an effective one-body one. This approximation is exact in the limit of a mean-field nuclear model, but can also be surprisingly accurate in more realistic calculations.

If we evaluate this effective operator for a spin- and isospin-symmetric core, the result is given diagrammatically by Fig. 2. The survival of a single contraction (and its time reverse)

$$\langle \beta | \hat{O}_{\rm eff} | \alpha \rangle = -\sum_{\substack{\sigma > F \\ \omega < F}} \left[\langle \omega | C1_N^5 | \sigma \rangle \frac{1}{E_\alpha + E_\omega - E_\beta - E_\sigma} \langle \beta\sigma | V_\rho | \omega\alpha \rangle + \langle \beta\omega | V_\rho | \sigma\alpha \rangle \frac{1}{E_\beta + E_\omega - E_\alpha - E_\sigma} \langle \sigma | C1_N^5 | \omega \rangle \right] \tag{15}$$

is due to a number of special properties of the operators. Because of its time reversal properties, $C1_N^5$ has no diagonal single particle matrix elements. Because the Simonius potential V_ρ carries charge, there are no particle-hole bubbles (with $C1_N^5$ entering on one end and V_ρ the other). And, as V_ρ vanishes when separately averaged to a one-body effective potential, all tadpoles at the ρ vertices vanish.

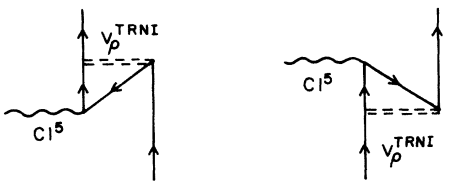

FIG. 2. The one-body effective operator representing the dominant axial coupling of the Z^0 ($J = 1$ projection of the axial charge) to a nucleus in its ground state. The TRNI is provided by an NN ρ-exchange potential.

In Ref. [8] we evaluated Eq. (15) in a spin- and isospin-symmetric Fermi gas model, with the simplifying assumption that the single-particle Green's functions appearing in Eq. (15) could be replaced by a constant energy denominator $\sim \hbar\omega$, the shell model oscillator spacing. The result was the effective TRNI PNC atomic potential

$$H(\mathbf{x}) = \frac{G}{\sqrt{2}} g_A (1 - 4\sin^2\theta_W) \frac{2}{15\pi^2} \mu_v g_\rho^2 \bar{g}_\rho \times \frac{k_F^5}{m_\rho^2 M^3} \frac{1}{\hbar\omega} \langle \mathbf{I} \rangle \cdot \nabla \delta(\mathbf{x}) \ . \tag{16}$$

This potential is identical in form to that for electrons interacting with a PNC TRNI nuclear EDM, once the effects of shielding [22] have been included

$$H_{\rm EDM}(\mathbf{x}) = -4\pi\alpha Q\frac{\langle \mathbf{I}\rangle}{I}\cdot\nabla\delta(\mathbf{x})\ , \tag{17}$$

where Q is the Schiff moment. A recent, very precise measurement of the atomic dipole moment $d_A(^{199}\mathrm{Hg})$ by Jacobs *et al.* [18],

$$|d_A(^{199}\mathrm{Hg})| < 1.3\times 10^{-27}\ e\ \mathrm{cm}\ (95\%\ \mathrm{C.L.})$$

then yields

$$|Q(^{199}\mathrm{Hg})| < 3.2\times 10^{-11} f^3\ .$$

Equivalently, for the interaction of Eq. (16), we find

$$|\bar{g}_\rho^{\rm eff}| < 3.2\times 10^{-3}\ (95\%\ \mathrm{C.L.})\ , \tag{18a}$$

where we have used $\sin^2\theta_W = 0.22$, $k_F = 280$ MeV, and $\hbar\omega = 41A^{-1/3}$ MeV=7.02 MeV. The notation "eff" signifies that this limit has been obtained in an independent particle model where the effects of short-range correlations on the ρ-exchange potential are omitted. To determine the corresponding limit on $\bar{g}_\rho$, we evaluated a series of shell model matrix elements of the Simonius potential for harmonic oscillator states near the proton and neutron Fermi seas, using both uncorrelated and correlated two-nucleon wave functions. The correlation function employed is that of Miller and Spencer [23]. Correlations reduce the rms matrix element by a factor of 2.9. Thus we conclude that the true TRNI meson-nucleon coupling has the weaker upper bound

$$|\bar{g}_\rho| < 9.3\times 10^{-3}\ (95\%\ \mathrm{C.L.})\ . \tag{18b}$$

VI. ATOMIC EDM'S ARISING FROM NUCLEAR PNC

A one-body nuclear EDM will be generated by the diagram of Fig. 1(a), where the nucleus can be visualized naively as the unpaired valence particle above a spin-paired nuclear core. However, calculations of nuclear EDM's generated by TRNI PNC interactions, such as the θ term in the QCD Lagrangian, suggest the possibility of a significant many-body enhancement of the nuclear EDM over its one-body scale [24]. To evaluate this possibility in the present case, we consider processes in which the nucleus couples to an external electric field because of the simultaneous polarization of the nuclear ground state by the interactions of Eqs. (3) and (5) [Fig. 1(c)].

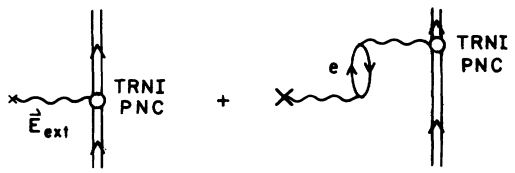

FIG. 3. Illustration of the screening of the direction interaction of the external field with a nuclear EDM by the polarization of the atomic cloud.

The task of estimating this second-order polarization contribution is quite formidable. Unlike the calculation in Sec. V, where the properties of the $C1_N^5$ operator limit the contributing TRNI polarization amplitudes to those with long wavelengths, high momentum intermediate states contribute to the nuclear EDM. [Note that the $C1_N^5$ operator, in a harmonic oscillator basis, generates transitions with $\Delta N = 0$ or 2, where N is the principal oscillator quantum number. Thus, while TRNI amplitudes with $\Delta N \gg 2$ are produced when V_ρ acts on the ground state, these do not contribute to the polarization sum of Sec. V.] In the case of the nuclear EDM, however, highly excited nuclear excited states can contribute between subsequent actions of V_ρ and $V^{\rm PNC}$, considerably complicating the calculation.

The direct interaction of a nuclear EDM with an external electric field is almost completely screened by the corresponding polarization of the atomic electrons, as illustrated in Fig. 3. The residual interaction depends on nuclear finite size effects and on hyperfine interactions, and can be expressed in terms of an effective electron-nucleus CP-odd interaction (in the interesting case of $S \leftrightarrow P$ atomic transitions):

$$H_{\rm eff}^{e-N} = -4\pi\alpha\frac{\langle \mathbf{I}\rangle}{I}\cdot\nabla\delta(\mathbf{x})[\ \langle\ \widehat{r^2 d}\rangle - \tfrac{5}{3}\langle\hat{r}_p^2\rangle\langle\hat{d}\rangle + \text{hyperfine corrections}]\ , \tag{19}$$

where $\langle\hat{d}\rangle$ is the ground-state expectation value of the nuclear dipole operator

$$\langle\hat{d}\rangle = \left(\frac{I}{(2I+1)(I+1)}\right)^{1/2}\left\langle I\left\|\int d^3y\,\mathbf{y}\hat{\rho}_H(\mathbf{y})\right\|I\right\rangle_{\rm TRNI,PNC}\ . \tag{20}$$

Here $\hat{\rho}_H(\mathbf{y})$ is the nuclear charge operator, the sum of the usual charge operator $[\hat{\rho}_0^H(\mathbf{y}) = \sum_{i=1}^A (1+\tau_3(i)/2)\delta(\mathbf{y}-\mathbf{r}(i))]$ and the TRNI one generated by the time component of the current of Eq. (7), $\mathbf{I}$ is the nuclear ground state spin, and $||$ denotes a matrix element reduced in angular momentum. The notation $\langle\rangle_{\rm TRNI,PNC}$ is a reminder that only TRNI PNC terms yield a nonvanishing contribution to the matrix element. These come from two sources. The combined action of $V_\rho^{\rm TRNI}$ and $V^{\rm PNC}$ in the nuclear wave function generate a nonzero matrix element of the $C1$ projection of $\hat{\rho}_0^H$, while the $C1$ projection of the TRNI charge operator corresponding to Eq. (7) is nonzero between unperturbed wave functions. The TRNI and PNC nuclear polarization contribution in the wave function is expected to dominate the dipole moment, and is all we consider in this section. The dipole moment is multiplied by the normalized second moment of the usual charge operator

$$\langle \hat{r}_\rho^2 \rangle = \frac{1}{Z}\frac{1}{\sqrt{2I+1}}\left\langle I \left|\left| \int d^3y y^2 \hat{\rho}_0^H(y) \right|\right| I \right\rangle . \quad (21)$$

The remaining TRNI operator of Eq. (19) is the second moment of the dipole density

$$\widehat{\langle r^2 d\rangle} = \frac{1}{\sqrt{(2I+1)(I+1)I}} \times \langle I|| \int d^3y y^2 \mathbf{y} \hat{\rho}_H(\mathbf{y}) ||I\rangle_{\mathrm{TRNI,PNC}} . \quad (22)$$

We note that quantity $[\widehat{\langle r^2 d\rangle} - \frac{5}{3}\langle \hat{r}_p^2\rangle\langle \hat{d}\rangle] \equiv Q$ is the Schiff moment discussed in Sec. V.

To determine the scale of the Schiff moment for ^{199}Hg that would arise from the combined effects of V_ρ^{TRNI} and V^{PNC}, we again appeal to effective operators. That is, we evaluate $\langle \hat{d}\rangle$ and $\widehat{\langle r^2 d\rangle}$ in a mean field picture in which the nuclear ground state is approximated as a single particle outside of a closed core. The effective operator corresponds to the contraction

$$\sum_{\alpha\beta}\langle\alpha|\hat{O}_{\mathrm{eff}}^{(1)}|\beta\rangle a_\alpha^\dagger a_\beta = \Bigg[\frac{1}{2}\sum_{\alpha_1\beta_1\gamma_1\delta_1}\langle\alpha_1\beta_1|V_\rho^{\mathrm{TRNI}}|\gamma_1\delta_1\rangle a_{\alpha_1}^\dagger a_{\beta_1}^\dagger a_{\delta_1} a_{\gamma_1} \frac{1}{E_{\delta_1}+E_{\gamma_1}-E_{\alpha_1}-E_{\beta_1}} \sum_{\alpha_2\beta_2}\langle\alpha_2|\hat{O}_1|\beta_2\rangle a_{\alpha_2}^\dagger a_{\beta_2}$$
$$\times \frac{1}{2}\sum_{\alpha_3\beta_3\gamma_3\delta_2}\frac{1}{E_{\delta_3}+E_{\gamma_3}-E_{\alpha_3}-E_{\beta_3}}\langle\alpha_3\beta_3|V^{\mathrm{PNC}}|\gamma_3\delta_3\rangle a_{\alpha_3}^\dagger a_{\beta_3}^\dagger a_{\delta_3} a_{\gamma_3}$$
$$+\text{other time orderings}\Bigg]_{\alpha\beta}^{\text{quadruply contracted}} , \quad (23)$$

where $\hat{O}_1$ represents the dipole and r^2-weighted dipole operators $\sum_{i=1}^A \frac{1}{2}\tau_3(i)\mathbf{r}(i)$ and $\sum_{i=1}^A r(i)^2\frac{1+\tau_3(i)}{2}\mathbf{r}(i)$ of Eqs. (20) and (22). [Note that the isoscalar dipole operator cannot cause intrinsic excitations: it is entirely spurious.] The contractions are performed by transforming to particle and hole operators relative to a Fermi sea, which for simplicity we chose to be spin and isospin symmetric. While the contractions are somewhat simpli-

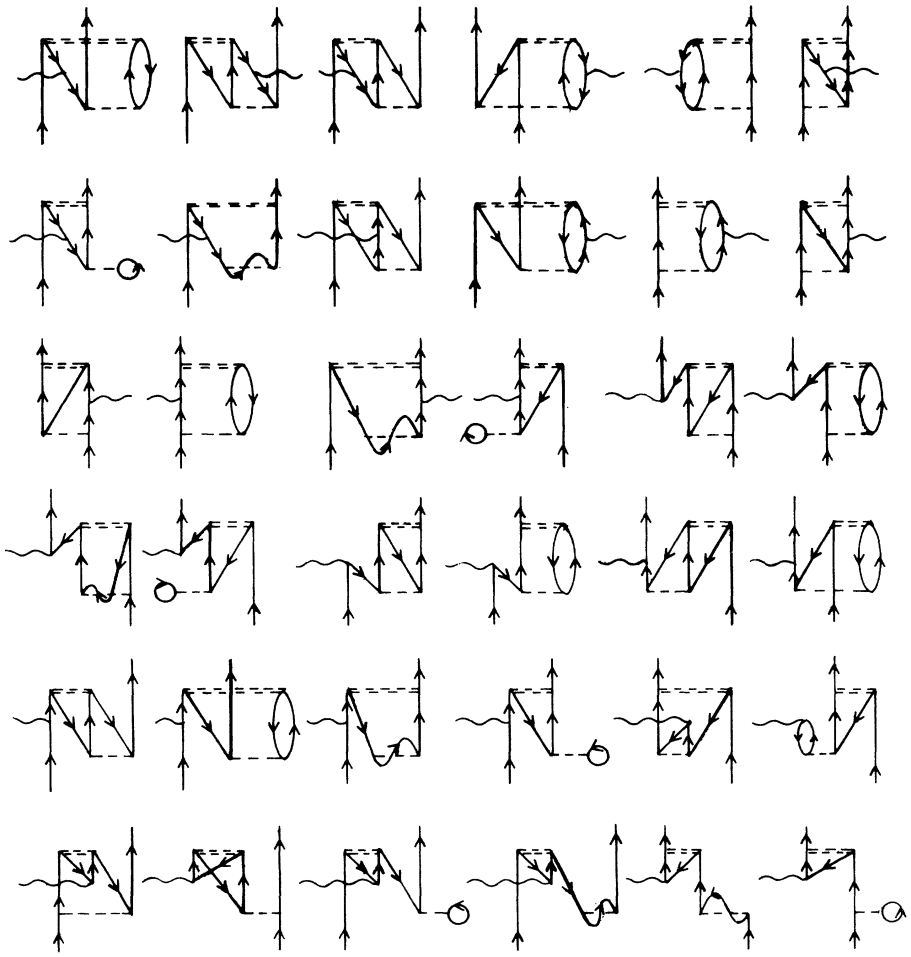

FIG. 4. Contributions to the one-body nuclear EDM of Eq. (23) corresponding to the time ordering where the external field acts between a PNC interaction (single dashed line) in the initial state and a TRNI interaction (double dashed line) in the final state.

fied by the properties of V_ρ [see the discussion following Eq. (15)], the evaluation of the full set of surviving terms is a formidable task. The 36 diagrams that survive for the operator ordering $V_\rho^{\rm TRNI}\hat{O}_1 V^{\rm PNC}$ are given in Fig. 4, while the corresponding diagrams for the effective TRNI PNC potential due to the time ordering $\hat{O}_1 V_\rho^{\rm TRNI} V^{\rm PNC}$ are given in Fig. 5.

The single-particle matrix elements corresponding to these diagrams were evaluated numerically in a harmonic oscillator basis by explicit summations over intermediate states. The harmonic oscillator is convenient because it provides a discrete basis as well as a nuclear size scale (the oscillator parameter) on which matrix elements of the dipole operators depend explicitly. The matrix elements of $V_\rho^{\rm TRNI}$ and $V^{\rm PNC}$ can be evaluated with the standard techniques of Brody-Moshinsky brackets and Talmi integrals [25]. We included in these matrix elements a two-nucleon correlation function [23] to account for the hard-core repulsion (or high-momentum interactions) absent in the shell model. The summations are convergent, but high-lying excitations must be included to obtain reliable results. We included particle excitations up to $12\hbar\omega \sim 170$ MeV above the Fermi sea, where we found the results were stable to $\lesssim 4\%$ when an additional shell was added.

We are primarily interested in ^{199}Hg, where the most restrictive EDM limit has been obtained. This is an odd neutron nucleus that can be described reasonably by a Nilsson model with small negative deformation, $\delta \sim -0.1$. The levels near the neutron Fermi surface have the $3p_{1/2}$, $3p_{3/2}$, and $2f_{5/2}$ shells as their spherical-limit parents. Thus we focused on Eq. (23) for low angular momentum states, l =0–3. To help make the calculations tractable, we chose relatively simple nuclear cores, evaluating the polarization sums for $2s_{1/2}$, $1d_{3/2}$, and $1d_{5/2}$ particles outside a ^{16}O core and for $2p_{3/2}$ and $1f_{5/2}$ particles outside a ^{40}Ca core. We chose oscillator parameters for these cores of $b = 1.7$ f and 1.86 f, values corresponding to realistic nuclear densities.

As the effective operator in Eq. (23) has $J = 1$, we know its exact magnetic dependence; we can also determine the exact isospin dependence from proton and neutron matrix elements. The goal of our work is to complete the characterization of an approximate, effective operator by deducing its form from a limited set of matrix elements. Helping us is the observation that as meson ranges are small compared to the nuclear size, the operator should depend on gross nuclear properties such

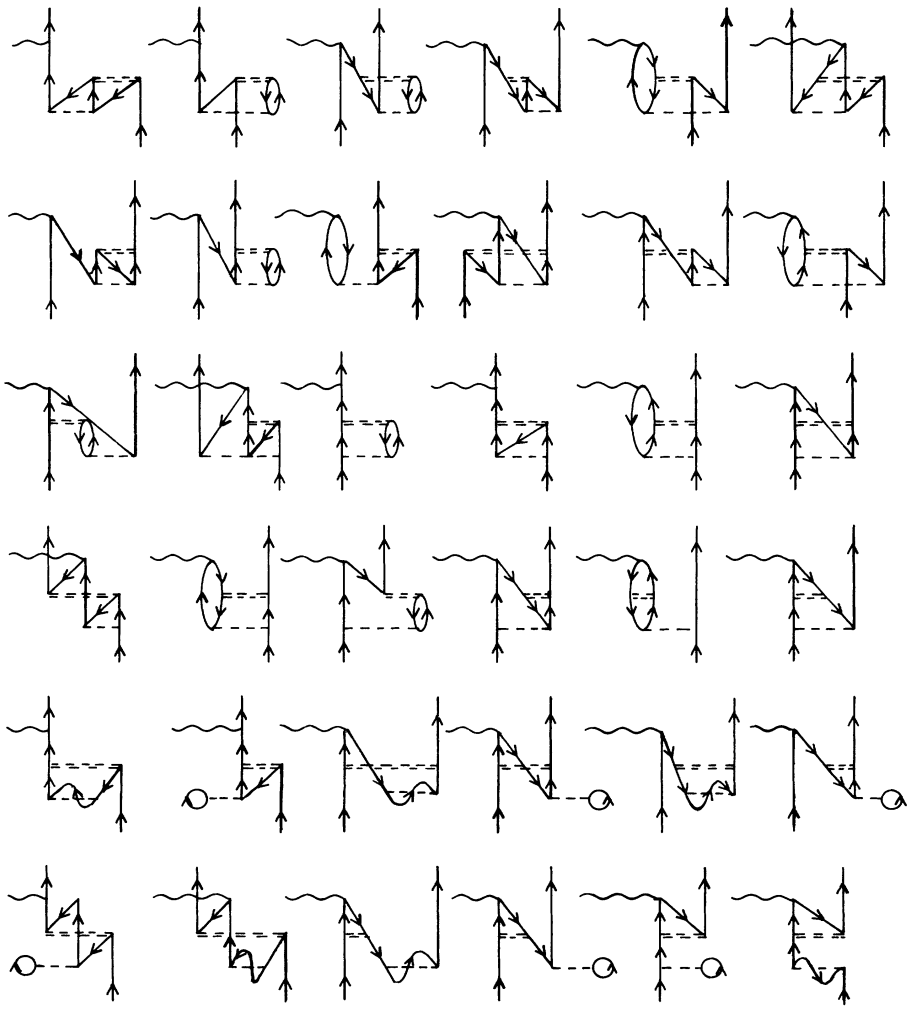

FIG. 5. As in Fig. 4, only for an effective TRNI PNC component in the initial state generated by subsequent PNC and TRNI polarizations. Only one time ordering of the intearctions is shown.

as the density, a quantity that varies only gently with mass number A.

The obvious spin-space operators having positive parity, $J = 1$, and no density dependence are $\boldsymbol{\sigma}_z(i)$ and $[Y_2(\Omega_i)\otimes\boldsymbol{\sigma}(i)]_{1z}$. The former is strongest in the stretched state ($j = l+s$), while the latter vanishes for $l = 0$ and is strongest for antiparallel states ($j = l-s$). The numerical results are very nicely represented by the latter,

$$\hat{d}_z^{\rm eff}(i) = (1.17\times10^{-8}f)\bar{g}_\rho[Y_2(\Omega_i)\otimes\boldsymbol{\sigma}(i)]_{1z}\left\{-\left[0.85\left(\frac{h_\rho^0}{h_\rho^{0\rm DDH}}\right)+0.021\left(\frac{h_\omega^0}{h_\omega^{0\rm DDH}}\right)\right]\right.$$
$$\left.+\left[\left(\frac{f_\pi}{f_\pi^{\rm DDH}}\right)+0.0022\left(\frac{h_\rho^1}{h_\rho^{1\rm DDH}}\right)+0.012\left(\frac{h_\omega^1}{h_\omega^{1\rm DDH}}\right)\right]\tau_3(i)\right\}, \quad (24)$$

where we have scaled the weak PNC couplings according to the best values of Ref. [11]. The overall coefficient of the f_π term ($1.17\times10^{-8}f$) varies by about $\pm20\%$ over the range of matrix elements studied; the overall coefficients of the vector meson contributions vary by less than $\pm10\%$. This effective operator predicts no s-wave strength, consistent with the numerical result that the matrix element for a neutron $2s_{1/2}$ transition is 0.086 that of a $1d_{3/2}$ transition. No ρ-exchange tensor term appears because it alone among the possible couplings was not well represented by a simple effective operator. [Note that its matrix elements were very small, so this is of no consequence numerically.]

In fact, all of the vector meson $\Delta I \neq 0$ PNC couplings make negligible contributions $\hat{d}_z^{\rm eff}$. [This result follows in part from the assumption of an isoscalar core. Corrections proportional to $(N-Z)/A$ will arise in a more general treatment. See Ref. [11] for an analogous, more general calculation in the case of PNC.] Clearly the strongest contributions come from h_ρ^0 and f_π in the case of an odd-neutron nucleus. Thus ^{199}Hg is a favorable case for constraining $\bar{g}_\rho$.

The calculation was repeated for the second operator of Eq. (19), $\widehat{r^2 d}$, with the pleasing and simple result

$$[\widehat{r^2(i)}d_z(i)]^{\rm eff} = 1.13r^2(i)\hat{d}_z^{\rm eff}(i)\ . \quad (25)$$

The uncertainty in the overall coefficient is $\pm10\%$; that is, each component in Eq. (24) scales in this way, with the variations in the scaling coefficient always lying within 10% of the average value 1.13.

Our approach was then to take this effective operator and embed it in a more realistic calculation for ^{199}Hg. We adopted the Nilsson model, using parameters for the valence shells taken from Gustafson *et al.* [26]. A deformation of $\delta = -0.1$ was used, placing the valence neutron in the $[Nn_Z\Lambda K] = [501\frac{1}{2}]$ orbit. The resulting transition density matrix then yields

$$\langle jj|\hat{d}_z|jj\rangle = (3.5\times10^{-10})\bar{g}_\rho$$
$$\times\left[0.85\left(\frac{h_\rho^0}{h_\rho^{0\rm DDH}}\right)+\left(\frac{f_\pi}{f_\pi^{\rm DDH}}\right)\right]b\ , \quad (26)$$

where $b \sim 2.43f$ is the oscillator parameter. Using the same model to evaluate $\langle\hat{r}_\rho^2\rangle$ and employing Eq. (25), it follows

$$Q(^{199}{\rm Hg}) = (-1.3\times10^{-9}f^3)\bar{g}_\rho$$
$$\times\left[0.85\left(\frac{h_\rho^0}{h_\rho^{0\rm DDH}}\right)+\left(\frac{f_\pi}{f_\pi^{\rm DDH}}\right)\right]. \quad (27)$$

Thus using the DDH best values, we conclude from the experiment result

$$|\bar{g}_\rho| < 0.013\ (95\%\ {\rm C.L.}) \quad (28)$$

a bound very similar to that found from the atomic PNC calculation of Sec. V.

VII. LIMITS ON $|\alpha|$ AND CONCLUSIONS

Direct tests of TRNI PC NN interactions have been made, following a suggestion by Wigner, in compound-nucleus studies of detailed balance and nuclear energy-level fluctuations. Limits are usually quoted in terms of the typical strength of TRNI PC nuclear matrix elements to those of the residual strong interaction, $\alpha = \langle H_{\rm TRNI\ PC}\rangle/\langle H_{\rm strong}\rangle$. From detailed balance studies in the region of overlapping compound-nucleus resonances, Boosé, Harney, and Weidenmüller [4] deduced

$$|\alpha| < 4\times10^{-3}\ (99\%\ {\rm C.L.})\ .$$

French *et al.* [5] studied spectral fluctuations and strength distribution in the regime of isolated resonances in the compound nucleus. From the spectral fluctuations they deduced

$$|\alpha| \lesssim 2\times10^{-3}\ (99\%\ {\rm C.L.})\ .$$

Finally, we note that the limit from the neutron transmission experiment exploiting the fivefold TRNI PC correlation [6] is

$$|\alpha| \lesssim 5\times10^{-3}\ (95\%\ {\rm C.L.})\ .$$

The connection between α and $\hat{g}_\rho$ can be established by considering NN matrix elements of the Simonius potential given in Eq. (5). These were evaluated for shells near the proton and neutron Fermi surfaces in ^{199}Hg ($2d_{3/2}$, $1h_{11/2}$, $1h_{9/2}$, $3p_{1/2}$, and $1i_{13/2}$) using a harmonic oscillator wave function characterized by $b = 2.43\ f$, as in Sec. VI. As in our earlier calculations, we modified the two-nucleon densities by a correlation function to take account of the short-range correlations missing from the shell model. The result, averaging 41 nonzero matrix el-

ements of $V_\rho(\mathbf{r})$ for $\bar{g}_\rho = 1$, is a rms matrix element of 3.6 keV. The scale of the matrix elements arises from the fact that TRNI ρ exchange is short-ranged ($m_\rho \gg k_F$, the Fermi momentum) and proceeds, in leading order in k_F, by $^1P_1 \leftrightarrow {}^3P_1$ transitions. Thus there is a natural suppression $\sim (k_F/m_\rho)^2 \sim 0.09$.

By evaluating corresponding strong interaction matrix elements for Serber-Yukawa and Rosenfeld potentials [27], we determined [8] that the corresponding scale for matrix elements of shell model residual interactions is ~ 300 keV. We then deduce, from Eqs. (11), (18b), and (28) the following bounds at 95% C.L.

$$|\alpha| \leq 10^{-5} \begin{cases} 0.64|f_\pi^{\mathrm{DDH}}/f_\pi| & \text{neutron}, \\ 11 & {}^{199}\mathrm{Hg}, \text{atomic PNC}, \\ \dfrac{16}{|0.46(h_\rho^0/h_\rho^{0\,\mathrm{DDH}}) + 0.54(f_\pi/f_\pi^{\mathrm{DDH}})|} & {}^{199}\mathrm{Hg}, \text{nuclear PNC}, \end{cases}$$

or equivalently

$$|\bar{g}_\rho| \leq 10^{-3} \begin{cases} 0.53|f_\pi^{\mathrm{DDH}}/f_\pi| & \text{neutron}, \\ 9.3 & {}^{199}\mathrm{Hg}, \text{atomic PNC}, \\ \dfrac{13}{|0.46(h_\rho^0/h_\rho^{0\,\mathrm{DDH}}) + 0.54(f_\pi/f_\pi^{\mathrm{DDH}})|} & {}^{199}\mathrm{Hg}, \text{nuclear PNC}. \end{cases}$$

The scale of the constraint from the neutron EDM limit is thus about 10^{-5}. Although we have evaluated only one of several possible hadronic loop diagrams in arriving at this constriant, and although it contains some uncertainty due to the loose experimental bounds on f_π, we nevertheless consider it to set the scale of the neutron EDM limit on $|\alpha|$ based on hadronic loops.

The limits from the EDM of ^{199}Hg, whether from atomic PNC or from nuclear PNC, are at $|\alpha| \lesssim 10^{-4}$, about a factor of 20 below the compound nucleus limits. There appears to be no loophole for avoiding these bounds. We note that, in contrast to the case where nuclear and atomic EDM's are induced by TRNI PNC interactions [24], the most stringent limits on TRNI PC physics appear to be generated by the neutron EDM.

Our bounds have been established for interactions of meson-exchange range. One expects TRNI to be generated at a more fundamental level by new weak interactions mediated by boson exchanges of very short range. This physics is buried within our effective coupling $\bar{g}_\rho$. The virtue of $\bar{g}_\rho$ as a starting point for TRNI PC phenomenology is that one can reliably relate this quantity to observables, and thus quantitatively compare the sensitivity of rather disparate experiments, such as TRNI PNC EDM measurements and direct compound nucleus tests of TRNI PC interactions. This has been the primary motivation for the work reported here.

For standard model interactions, such as hadronic parity violation, one has a theory for relating underlying boson couplings to those of mesons and nucleons. While for hadronic PNC this relation is somewhat complicated by strong interaction corrections, one has some confidence that meson-nucleon couplings can be estimated to within factors of (1–3) [9]. The situation with PC TRNI interactions is quite different. As Herczeg, Kambor, Simonius, and Wyler have shown [2], a general feature of renormalizable gauge theories with elementary quarks is the absence of flavor-conserving TRNI PC interactions that are first order in the boson exchange between fermions.

Nevertheless, in analogy with the introduction of $\bar{g}_\rho$ at the meson-nucleon level, one can assume an effective TRNI PC derivative boson-quark coupling. Using such a starting point, Khriplovich [28] has made a dimensional estimate of the one-loop weak radiative corrections through which an EDM could be generated. By equating the scale of the radiatively induced TRNI PNC quark-gluon coupling to neutron/atomic EDM's, he estimates a bound on the TRNI PC boson-fermion coupling of $\lesssim 10 G_F m_\pi^2 \sim 10^{-6}$, a scale comparable to our neutron EDM limit on α.

Later Conti and Khriplovich [10] argued that representative two-loop corrections would permit the weak interaction to contribute at full strength and thus be enhanced by a factor of $\alpha/|G_F m_\pi^2| \sim 10^5$, relative to the one-loop corrections. This is clearly a short-range mechanism distinct from those we have considered here because the two-loop contribution cannot be factored into a product of weak PNC and TRNI PC interactions separated by low-momentum states. Thus these bounds are not in contradiction to our less restrictive results for long-range mechanisms. In Ref. [10] two classes of two-loop diagrams are considered, corresponding to an attachment of a gluon or photon, respectively. The former could contribute to a long-range nuclear interaction of a different sort, associated with an induced TRNI PNC vertex. The most restrictive bounds, which are derived from Fig. 1(a) of Ref. [10], then limit TRNI PC quark-quark interactions that carry color. Limits from the remaining diagrams [Figs. 1(b) and 1(c)] are about an order of magnitude weaker, but constrain colorless TRNI PC interactions. The diagrams involving the attachment of a photon generate a quark EDM; here Fig. 1(a) contributes for a colorless TRNI PC interaction.

These contributions involve a sum over fermions in a closed fermion loop. Since fermions are assumed to be massless in the calculations of Ref. [10], the amplitude for a single fermion carries no fermion mass dependence. Thus, taking Figs. 1(b) and 1(c) as an example, the only dependence on the species of fermion enters via the product of the virtual fermion's axial vector coupling to the Z_0 and its coupling to the X boson, which mediates the TRNI PC quark-fermion interaction. Thus it is possible,

depending on one's model for the latter coupling, that the sum over fermions within a given generation may vanish, in a manner analogous to the cancellation responsible for Glashow-Iliopoulos-Maiani (GIM) suppression of the $K_L - K_S$ mass difference. Until a model for the X-quark interaction is specified and a complete two-loop calculation performed, it is difficult to assess the plausibility of such a scheme for avoiding the low-energy consequences of these two-loop contributions.

In conclusion, we have considered neutron and atomic EDM's that could arise from weak radiative corrections to TRNI PC interactions of meson exchange range. We were able to make quantitative connections between these indirect tests of TRNI PC interactions and the direct ones based on detailed balance. The former appear to be more restrictive by about two orders of magnitude. Thus it would seem that direct tests of TRNI PC interactions, such as those performed in compound nuclei, cannot compete with the indirect constraints imposed by the limits on neutron and atomic EDM's.

ACKNOWLEDGMENTS

We thank Peter Herczeg for helpful discussions. This work was supported in part by the U.S. Department of Energy. M.J.M. was supported by the National Science Foundation Young Investigator Program.

[1] See, for example, P. Herczeg, in *Tests of Time Reversal Invariance in Neutron Physics*, edited by N. R. Robertson, C. R. Gould, and J. D. Bowman (World Scientific, Singapore, 1987), p. 24; E. M. Henley, in *ibid.*, p. 1.

[2] P. Herczeg, J. Kambor, M. Simonius, and D. Wyler, "Parity conserving time reversal violation in flavor conserving quark-quark interactions," Los Alamos Theory Division report (unpublished); P. Herczeg, Hyp. Interact. **75**, 127 (1992).

[3] E. Blanke, H. Driller, W. Glöckle, H. Genz, A. Richter, and G. Schrieder, Phys. Rev. Lett. **51**, 355 (1983); A. Richter, in *Interaction Studies in Nuclei*, edited by H. Jochim and B. Ziegler (North-Holland, Amsterdam, 1975), p. 191.

[4] D. Boosé, H. L. Harney, and H. A. Weidenmüller, Phys. Rev. Lett. **56**, 2012 (1986); Z. Phys. A **325**, 363 (1986).

[5] J. B. French, V. K. Kota, A. Pandey, and S. Tomsovic, Phys. Rev. Lett. **54**, 2313 (1985); Ann. Phys. (N.Y.) **181**, 198 (1988); R. U. Haq, A. Pandey, and O. Bohigas, Phys. Rev. Lett. **48**, 1086 (1982); J. B. French, V. K. B. Kota, A. Pandey, and S. Tomsovic, Ann. Phys. (N.Y.) **181**, 235 (1988).

[6] J. E. Koster *et al.*, Phys. Lett. B **267**, 23 (1991).

[7] See, for example, L. Wolfenstein, Nucl. Phys. **B77**, 375 (1974).

[8] Some results in this paper were reported earlier by W. C. Haxton and A. Höring, Nucl. Phys. **A560**, 469 (1993).

[9] B. Desplanques, J. F. Donoghue, and B. R. Holstein, Ann. Phys. (N.Y.) **124**, 449 (1980).

[10] R. S. Conti and I. B. Khriplovich, Phys. Rev. Lett. **68**, 3262 (1992).

[11] See A. Adelberger and W. C. Haxton, Annu. Rev. Nucl. Sci. **35**, 501 (1985).

[12] Note that Bjorken and Drell conventions are used. Thus γ_5 is minus that of Ref. [9].

[13] P. Herczeg, Nucl. Phys. **75**, 655 (1966).

[14] M. Simonius, Phys. Lett. **58B**, 147 (1975).

[15] E. C. G. Sudarshan, Proc. R. Soc. **A305**, 375 (1968); R. Bryan and A. Gersten, Phys. Rev. Lett. **26**, 1000 (1971); **27**, 1102 (1971); J. Binstock, R. Bryan, and A. Gersten, Phys. Lett. **48B**, 77 (1974); M. Simonius and D. Wyler, Nucl. Phys. **A286**, 182 (1977).

[16] K. F. Smith *et al.*, Phys. Lett. B **234**, 191 (1990).

[17] I. S. Altarev *et al.*, Phys. Lett. B **276**, 242 (1992).

[18] J. P. Jacobs, W. M. Klipstein, S. K. Lamoreaux, B. R. Heckel, and E. N. Forston, Phys. Rev. Lett. **71**, 3782 (1993).

[19] B. Holzenkamp, K. Holinde, and J. Speth, Nucl. Phys. **A500**, 485 (1989).

[20] K. Ohta, Phys. Rev. C **40**, 1335 (1989).

[21] M. J. Musolf and M. Burkardt, Z. Phys. C **61**, 433 (1994).

[22] L. I. Schiff, Phys. Rev. **132**, 2194 (1963).

[23] G. A. Miller and J. E. Spencer, Ann. Phys. (N.Y.) **100**, 562 (1976).

[24] G. Feinberg, Trans. N.Y. Acad. Sci. **38**, 6 (1977); W. C. Haxton and E. M. Henley, Phys. Rev. Lett. **51**, 1937 (1983); V. V. Flambaum, I. B. Khriplovich, and O. P. Sushkov, Zh. Eksp. Teor. Fiz. **87**, 1521 (1984) [Sov. Phys. JETP **60**, 873 (1984)]; Phys. Lett. **162B**, 213 (1985); Nucl. Phys. **A449**, 750 (1986).

[25] T. A. Brody and M. Moshinsky, *Tables of Transformation Brackets for Nuclear Shell-Model Calculations* (Gordon and Breach, New York, 1967).

[26] C. Gustafson, I. L. Lamm, B. Nilsson, and S. G. Nilsson, Ark. Fys. **36**, 613 (1967).

[27] A. deShalit and H. Feshbach, *Theoretical Nuclear Physics* (Wiley, New York, 1974), Vol. 1, p. 373.

[28] I. B. Khriplovich, Nucl. Phys. **B352**, 385 (1991).